TECHNICAL APPROACHES FOR HIGH AVERAGE POWER FELS

George R. Neil
Thomas Jefferson National Accelerator Facility (Jefferson Lab), 12000 Jefferson Avenue,
Mail Stop 6A, Newport News, VA 23606, USA

Abstract

High power Free Electron Laser (FEL) oscillators have only recently achieved their original promise as producers of high power short wavelength tunable radiation. Room temperature accelerator systems limited duty factor and the ability to carry high brightness beam, and also increased the cost of RF power drivers in covering cavity wall losses. The application of SRF technology has now permitted more than two orders of magnitude increase in FEL average power just due to increased duty factor. A concurrent key technical development that leveraged the high efficiency of SRF linacs was the demonstration of beam energy recovery while lasing. This leads to high overall efficiency and scales favorably to even higher average power systems. This paper will discuss the issues relating to high average power FELs utilizing the results of the IR Demo FEL at Jefferson Lab to illustrate the sizeable advantages that SRF offers for multi-kilowatt average power output.

1 INTRODUCTION

Free Electron Lasers place stringent demands on the electron beams produced by driver accelerators. The electron energy must be high to deliver wavelengths as set by the basic FEL resonance equation.

$$\lambda_s = (\lambda_w/2\gamma^2)(1+K^2) \qquad (1)$$

where λ_s is the output wavelength, λ_w the wiggler wavelength, γ the relativistic factor, and K is the wiggler strength parameter. $K = 0.934\, B_{rms}(T)\, \lambda_w(cm)$ with B_{rms} the wiggler field. Achievable values of field for a given gap depend on the type of wiggler and wavelength with electromagnetic wigglers typically winning for wavelengths longer than around 5 cm and hybrid permanent magnet wigglers producing higher Ks for wavelengths shorter than 5 cm due to the difficulty in cooling the coils in electromagnetic wigglers. [1]

The FEL requires high peak currents in order to achieve sufficient gain to lase. This charge must be delivered with minimal degradation of the transverse and longitudinal emittances if the high gain is to be preserved. This design challenge becomes especially acute at short wavelengths. The small signal gain of the FEL is given by [2]

$$G = 29.4\, (I/I_A)(N_w^2/\gamma)B\eta_l\eta_f\eta_\mu \qquad (2)$$

where I is the current, I_A is the Alfven current = 17 kA, N_w is the number of wiggler periods, $B = 4\xi[J_0(\xi)-J_1(\xi)]^2$ where $\xi = K^2/[2(1+K^2)]$. The last three terms (η_l, η_f, η_μ) account for emittance and energy spread effects, gain degradation due to imperfect beam overlap, and slippage between the electrons and the optical pulse.

What gain is desirable? That is set in high power oscillators by the amount of power that mirrors can take since the power circulating in the cavity is inversely proportional to the out-coupling for a fixed output power. When operation at the kilowatt level and above is considered the mirror distortions introduced by high average power can be limiting unless the best possible materials and coating technologies are used [3]. It is always desirable to maximize the outcoupling fraction consistent with having the saturated gain sufficiently high to provide extraction efficiencies of $1/4N_w$. For stable operation and optimum efficiency one typically designs the oscillator to have an out-coupling of about 1/3 the small signal gain.

Given this scaling there are several approaches taken to optimize the system. One can see that Eq. 2 suggests increasing the peak current, increasing the magnetic field of the wiggler, and lowering the beam energy to increase gain. Each of these has its own limitation which prevents arbitrary increases in the gain. The maximum peak current that can be achieved is set by the longitudinal emittance of the electron beam and the charge in the bunch. It is now commonplace to perform bunching of the electron beam by riding off the peak of the rf phase thus providing an energy slew to the electron micropulse and then sending the beam through chicane with a path length/energy correlation. If the higher energy electrons can be arranged to take a shorter path through the chicane then they can catch up with the earlier, lower energy electrons by the exit of the chicane and produce a short pulse of high peak current. This can produce sizeable peak currents; multi-kiloamps are planned for the LCLS device in a 200 fs pulse. Ultimately this is limited by the intrinsic energy spread present in the beam before the bunching occurred or non-linearities in either the rf field or magnetic transport.

Increasing the wiggler field drives one to longer wavelengths through the requirements of Eq. 1 unless the energy is also increased which goes opposite to what one desires if the goal is to increase the gain. For high average power FELs shortening the wiggler wavelength until K is about one provides a near optimal situation for gain at the fundamental wavelength. The option of using microwigglers is considered risky in high power FELs

because of the need to get very high average currents through the wiggler vacuum chamber without scraping. Experience at Jefferson Labs suggests that the electron beam loss goes like the local beta (envelope function) of the matched electron beam in the wiggler divided by the aperture [4]. Thus a good starting point for a high power design is to assume K = 1 and for a desired output wavelength one gets a ratio of (λ_w/γ^2) which one can subject to the above criteria: ability to make K ~ 1 at the desired lasing wavelength. There are two factors which may push the designer to higher beam energies. One is the desire for higher beam power; it is equal to the product of the average current and the beam energy. The second is the need to minimize degradation of gain by finite emittance effects.

The last three terms in Eq. 2 are all equal to one for perfect electron beams. They account for effects of finite energy spread, and emittance. For optimum coupling to occur the optical beam must overlap the electron beam through the wiggler. In addition, due to finite emittance the betatron motion of electrons in the wiggler causes them to sample variations in the wiggler field leading to an effective energy spread. This sets a soft limit on the emittance ε of the electron beam for achieving a particular wavelength given by

$$\varepsilon < \lambda/4\pi\,, \quad (\lambda/4\pi)(\beta/L_{1D}) \tag{3}$$

for oscillators [2], and amplifiers [5]. Here β is the matched envelope function of the wiggler and L_{1D} is the 1 dimensional gain length. Since this emittance is equal to the normalized emittance divided by γ, one can, in principle, get to shorter wavelengths by increasing the beam energy to alleviate this restriction.

Likewise the gain of the FEL falls off if the energy spread is too large in both oscillators and amplifiers because the electrons tend to fall out of resonance with the pondermotive wave.

$$dE/E < 1/(4\pi N_w)\,, \ (1/4\pi)(L_{1D}/\lambda_w) \tag{4}$$

These criteria, though soft, allow for the choice of FEL accelerator performance from essentially first principles.

Additional performance goals are often set by the FEL linac designer. For a useful device the designer wants exceptional wavelength stability which translates directly into linac energy stability (the wavelength moves 2% for every 1% energy shift). There are also phase stability requirements of the beam at the wiggler which set stability limits on the master oscillator system, the rf phase control, and through dispersive path length coupling, the beam energy stability. Treatment of these is beyond the scope of this article except to say that CW operation of the linac generally offers advantages in phase and amplitude control for stability. We refer the reader to [6].

The designer of such a linac system often wants these qualities at high duty factor, either to achieve high average power or to supply light to many different users through a switching system. Superconducting rf technology is uniquely suited to provide an answer to these requirements and provide additional benefits besides. We discuss these design drivers in depth below, provide some scaling arguments, and then illustrate their implication by example of their application to one system already operational and one planned.

2 LINAC DESIGN CHOICES

In choosing a linac technology – copper or srf – for an FEL linac there are both physics issues and system level design factors which lead one to the srf approach when high power or high duty factor is desirable. In this regard the design drivers for high power FELs are similar to those of other high current systems such as B factories and reviews such as [7] offer excellent guidance in design choices. The physics issues to consider include beam breakup (BBU) instabilities, wakefield generation, and beam energy and phase stability. The system level design drivers include the ability to operate CW for high duty factor and/or high average power, and the ability to incorporate energy recovery for reduced capital investment, higher operating efficiency and reduced operating costs. We will treat the physics issues first.

2.1 Physics Issues

Every relativistic beam transport system causes some degradation to the electron beam quality. It is important to ensure that this degradation does not lead to a significant reduction in performance of the FEL. As was shown above there are fairly sharp cliffs beyond which good performance of the FEL is exceedingly hard to obtain. While one cannot state with certainty that a particular design choice cannot be made to meet a set of energy spread or emittance criteria there are guidelines which suggest the direction one should go to make it easier to meet them.

One effect which causes an increase in energy spread of the micropulses is longitudinal wakefields which occur any time a relativisic beam passes through an aperture or change in pipe diameter. The effect scales like

$$dE \sim Q N_{cavities}\,(g N_{cell}/\sigma)^{1/2}/a \tag{5}$$

where $N_{cavities}$ is the number of accelerator cavities in the linac, N_{cell} is the number of cells per cavity, g is the gap, a the aperture, and σ is the RMS micropulse length of the charge Q [8].

While the micropulse length has no particular dependence on whether the design is copper or srf, the other terms do depend on this. To reach a particular energy requires a certain number of cavities operating at a particular gradient. We have chosen a specific copper cavity design and a srf cavity design from [7] to illustrate the frequency dependencies. For this comparison the HOM loading of a copper cavity was 0.34 V/pC while an identical frequency srf cavity was 0.11 V/pC. Since the

shunt impedance is not such a design driver for srf cavities much larger apertures are generally used. The fundamental R/Q was 265 Ohm/cell for the copper cavity and 89 Ohm/cell for the SRF cavity. It is assumed that the cavity geometry scales with frequency although physically it is easier to damp HOMs in larger structures.

The maximum gradient achievable depends on frequency and whether the system is pulsed or CW. For copper systems operating CW the gradient limit is set by the cooling capability so the heat flux was held constant as frequency was varied. This results in gradient scaling as $(\text{frequency})^{1/4}$. In pulsed operation the gradient limit is field emission which has an entirely different dependence. The operational limits are generally chosen as some factor times the Kilpatrick limit [9], E_{kp} given by (in transcendental form with E_{Kp} in MV/m and f in MHz)

$$f = 1.64\, E_{Kp}^{\ 2}\, e^{-(8.5/E_{kp})} \qquad (6)$$

This typically drives CW copper machines to low frequency and pulsed machines to as high a frequency for which the beam will remain stable. A known operating value of 3 MV/m at 405 MHz for CW and 50 MV/m pulsed at 2700 MHz set the absolute scales. Higher values have caused erosion of the cavity [10].

For the SRF cavities different factors come in to play and in the past the scaling limits for an ensemble of cavities have been dominated by surface imperfections when operating CW [11]. Empirically, the gradient scales as $(\text{surface area})^{-1/4}$. Significant differences are often found between single cell cavities at a particular frequency and multi-cell cavities. Reductions in operating gradient are also invoked between vertical test stand data and beam operations in horizontal cryostats. As surface cleaning techniques and the quality of niobium have improved, these scaling limits have become less clear. There are many examples now of high gradient cavities at low frequencies which exceed previously believed limits by substantial margins (Fig. 1). There should still be improvement as one goes to higher frequencies and so we have conservatively chosen a linear scaling with frequency to illustrate the beam scaling factors. As more data becomes available and the true limits appear these curves should be updated appropriately.

The difference in limits between pulsed and CW are not as clearly established as in the case of copper machines but factors of two differences between CW and pulsed operation have been seen. It seems likely that srf cavities are subject to Kilpatrick limits just as copper machines are although the care with which srf cavities are generally treated and the excellent vacuum environment suggests that different safety factors may be applied. There is only a small amount of experiential data available so a value of 1/2 the pulsed gradient limit of copper cavities at the same frequency was used. One example is the TTF design value of 24 MV/m for their 9-cell 1300 MHz cavity. A pulsed copper cavity at this frequency could operate at 55 MV/m. This choice should also be revisited as further data becomes available. Care should be used in applying these results since there are many cavity operating condition dependent parameters that could materially affect the results. Nonetheless it is a useful starting point for system trades. Figure 1 shows the gradient limits assumed in the stability illustrations which follow.

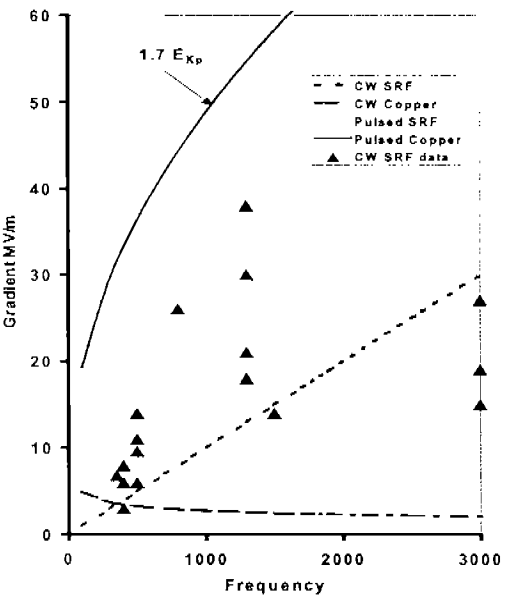

Figure 1: Gradient limits for pulsed and CW copper and srf linacs assumed in the stability calculations below with some illustrative recent srf results.

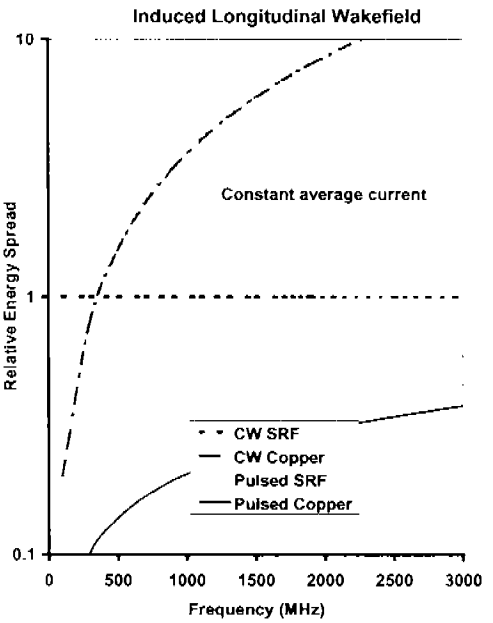

Figure 2: Longitudinal heating limits as a function of frequency. The scaling has assumed a fixed total energy, <I>, R/Qs for each system are the values quoted above, and micropulse length and cavity geometry ~ 1/f.

Figure 2 shows the frequency scaling for copper and srf machines operating pulsed or CW. It is clear from the curves that no particular advantage for srf exists if operating at low duty factor due to the high gradients that copper machines can achieve. Operating CW brings a sizeable competitive advantage to srf linacs in terms of minimizing beam degradation by longitudinal effects.

The transverse wakefield scales like [8]

$$dE \sim (Q/a^3)(g\sigma)^{1/2} L_{acc} / [\, l_{cell} \sqrt{N_{cell}}] \qquad (7)$$

up to $N_{eff} = ka^2/l_{cell}$

L_{acc} is the linac length, and l_{cell} is the cell length.

Figure 3 illustrates the results of this scaling versus frequency. Again there is no particular advantage to srf operating pulsed. In CW operation the copper cavities can never overcome the severe handicap given by the small apertures in the system.

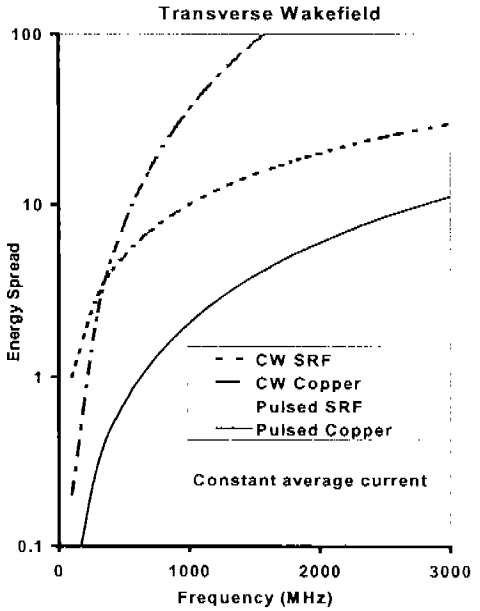

Figure 3: Transverse heating limits as a function of frequency.

The last physics parameter we consider is BBU. The specific threshold for regenerative BBU to occur is lattice dependent but that decision is essentially independent of copper versus srf technology and so is ignored. We also ignore pulsed systems since regenerative BBU has little time to grow in a pulsed system. Moreover recirculating a pulsed beam generally offers little advantage. The estimated threshold for BBU is [8]

$$I_{th} \sim 1/[\omega^2 \times L_{acc} \times Q_{HOM}] \qquad (8)$$

up to N_{eff}, as in Equation 7.

Here the benefit in length and Q_{HOM} by 3x each again gives nearly an order of magnitude benefit to srf operating CW as shown in Figure 4. It is also clear from Figures 2 - 4 that if CW operation is desired then there is a significant push toward lower frequencies if stable operation is essential. At the lowest frequencies copper cavities become competitive in terms of physics performance although the cost penalties paid for the rf wall losses in CW operation are large.

2.2 System Implications

It is apparent from the above discussion that for an equivalent design, the srf machine offers the potential of a cleaner beam or equivalently can transport a larger current. This capability may be put to effective use in the

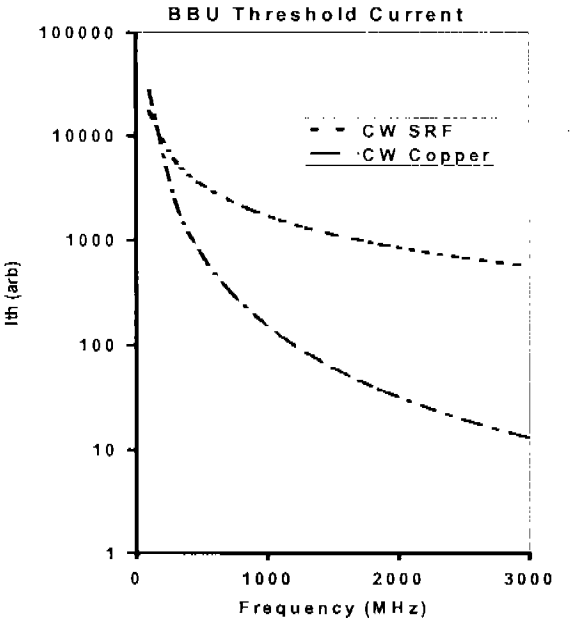

Figure 4: BBU limits as a function of frequency.

machine layout by recirculating the beam to higher energies in one linac (the approach that CEBAF uses to get 5 GeV beam from 1000 MeV of linac) or operating the second pass 180 degrees out of phase to decelerate the beam and convert its power back to RF energy. Such a technique was used with FEL lasing in a copper accelerator but utilizing a second accelerator to decelerate the beam and couplers to feed the energy back to the first structure [12]. Instabilities were observed under some operating conditions. The technique of same cell energy recovery has also been demonstrated without lasing [13] and more recently while lasing [14]. The implications of such an approach are best illustrated by example from the Jefferson Lab IR Demo.

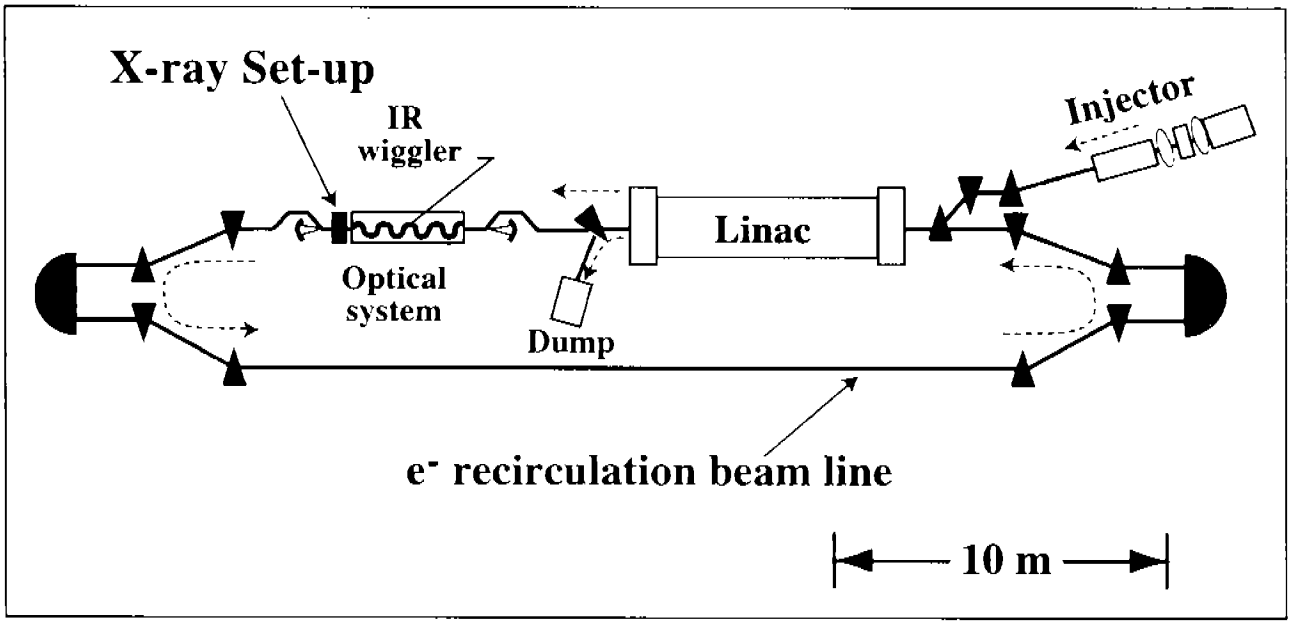

Figure 5. A layout of the IR Demo FEL. We also show a setup recently used to generate high fluxes of Thompson scattered X-rays in the 5 to 15 keV range produced when the FEL pulse scatters off the subsequent electron bunch. Up to 10^9 photons /sec were produced [15]

2.3 Implications of using same cell energy recovery

A schematic representation of the infrared demonstration FEL (IR Demo FEL) is shown in Fig. 5. The FEL is placed at the exit of the linac, the electron beam is deflected around the two optical cavity mirrors and then has two possible paths. One is straight ahead into a beam dump used for initial commissioning and tune up. The other is into a recirculation loop based on the isochronous achromats used in the Bates accelerator [16]. This latter path allows the electron beam to be recirculated for energy recovery and decelerated to a 10 MeV dump [17,18]

The motivation to use energy recovery as a key feature in the IR Demo design was to demonstrate the efficient and cost effective scalability of the system to yet higher average power [19]. Because of the low electron beam energy (48 MeV) it does not yet substantially improve the wall plug efficiency (only 2x to 3x). The tables below

Table 1: IR Demo AC Wall Plug Powers

	With ER	Without ER
Injector RF	220 kW	220 kW
Linac RF	175 kW	700 kW
He refrigerator	70 kW (est.)	70 kW (est)
Magnets, Computers, etc.	43 kW	23 kW
Total	**508 kW**	**1013 kW**

show measured and projected AC power consumption on the system. It should be emphasized that the following systems have not been optimized for low power consumption. In particular, the use of 1497 MHz low power klystrons has significantly penalized the overall wallplug efficiency. The present klystrons have an efficiency of 35% at their design power of 5 kW but use full bias power even when only providing the 2 kW or so to each cavity that the FEL requires in energy recovery mode. The use of an inductive output tube (IOT) at lower frequency would not only allow higher efficiency at full power but also only draw input power as required for the desired output. The overall AC draw for rf power would be markedly reduced. (Higher capital cost and lower achievable gradients would be associated disadvantages though.)

In the absence of energy recovery the AC power for linac RF would have been increased by 500 to 900 kW at the same efficiency achieved in the injector RF supply. Energy recovery has thus improved system performance by 58% to 64%. The benefits will be even more striking at higher beam energies and powers shown in Table 2. For a scale-up to 10 mA, 160 MeV, energy recovery will improve system performance by roughly 78%, reducing power draw from ~ 4700 kW to ~1075 kW. The required RF generation will be reduced by over 1700 kW saving on the order of $ 5M in capital costs. These factors become even more dominating as the power of the FEL grows to the very high levels required for an industrially useful device (~ 100 kW) resulting in excess of 6% wallplug efficiency for cost effective operation.

Table 2: IR Upgrade and 100 kW Industrial Prototype AC Wall Plug Powers

	Upgrade With ER	Upgrade Without ER	Prototype With ER
Injector RF	350 kW	350 kW	750 kW
Linac RF	525 kW	4200 kW	650 kW
He refrigerator	100 kW (est.)	100 kW (est.)	100 kW
Magnets, Computers, etc.	100 kW	40 kW	100 kW
Total	**1075 kW**	**4690 kW**	**1600 kW**

The use of energy recovery brings additional benefits to the IR Demo beyond reducing the rf capital cost and improving the system electrical efficiency:
1) it reduces the dissipated power in the beam dumps by > 4x. The electron beam is transported with virtually no losses to the dump so the power that must be handled on the dump face is reduced by the energy ratio (10 MeV/48 MeV = 0.21) times to 50 kW from 240 kW. In a higher power accelerator, say 10mA at 160 MeV, this advantage is even more striking: a reduction to 100 kW from 1600 kW.
2) it virtually eliminates induced radioactivity in the dump region by dropping the terminal energy below the photo-neutron production threshold. For a copper beam dump reducing the energy to below 10 MeV can essentially eliminate the neutron production which activates surrounding components. Operating experience on the IR Demo has radiation backgrounds during energy recovered running reduced by 10^4 or more. This increases lifetimes of electronic components and significantly impacts the ease with which system maintenance can be performed.

However, there were several technical issues that had to be addressed to take advantage of such an energy recovery approach: stability of the electron beam, stability of the lasing process in such an energy recovered system, management of transport of large energy spread beams with low beam loss, and minimization of coherent synchrotron radiation induced emittance growth. These were all successfully handled by design optimizations as discussed in the references [20,21,22]. The cost of the recirculation arcs, while significant, are less than rf savings.

2.4 Implications of CW operation

Operation in a continuous wave mode is natural for srf systems. The low wall losses and large Qs mean the small penalties in providing refrigeration for operating a machine CW are offset by the relative ease with which CW rf can be generated and controlled with feedback. In comparison to typical copper machines which operate at 10^{-3} duty factor, operating CW can provide sizeable increases in FEL output power without invoking new laser physics. This is best illustrated by Figure 6 which

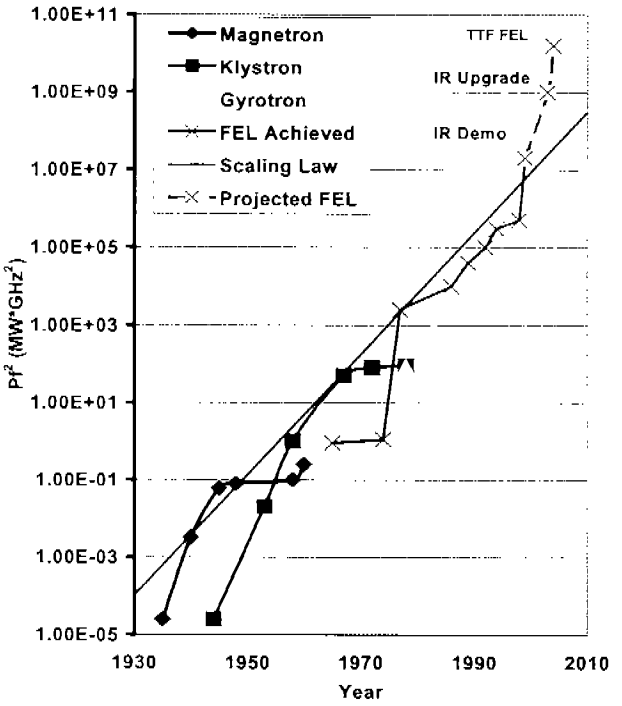

Figure 6: A time history of progress in electron operated radiation devices. Projected performance of the IR Upgrade and the TTF FEL is also shown. Adapted from [23].

shows the operation barrier reached by FELs before invoking CW operation in srf machines. Such a breakthrough in technical approach is expected to produce not only further advances above the line of typical development but in the reasonably near future a 4th generation X-ray User facility providing light to many end stations at fluences 5 orders of magnitude or more higher than available today. The scientific possibilities are enormous.

3 WORLD SRF FEL FACILITIES

Table 3 lists the operational and planned srf FEL facilities around the world. Progress in this area has been steady and encouraging. There are now five operational srf facilities around the world and of those two are User facilities where outside researchers can perform photonics research using the FEL. Substantial advantages are gained through the use of the srf technology in applications directed toward user facilities. To gain insight into the capabilities we discuss below an example: a state of the art facility in the infrared, the Jefferson Lab IR Demo in Virginia.

Table 3. World SRF FEL Facilities
Those initalics are under construction or commissioning. See [24] for references on each system.

Country	Institution	Device	λ(μm)	τ_p(ps)	E_b/I_b (MeV/A)	P_{peak} (MW)	P_{avg} (W)	Accelerator freq. (MHz)
USA	Stanford U	FIREFLY	19-65	1-5	20/14	.3	.4	1300 Pulsed (CW)
		SCA/FEL	3-10	0.5 - 12	37/10	10	1.2	1300 Pulsed (CW)
	JLab	IR Demo	3-8	0.6-2	48/60	25	1700	1497 CW
		IR Upgrade	*.2-25*	*0.5-2*	*160/100*	*150*	*10000*	1497 CW
Germany	*Rossendorf*	*ELBE*	*5-150*	*1-2*	*40/50*			*1300 CW*
	DESY	*TTF FEL*	*0.04-0.2*	*.8*	*390/500*	*2000*	*7200*	*1300 Pulsed*
	Darmstadt	S-DLINAC	6-8	2	50/2.7	.15	3	3000 CW
Japan	JAERI	SCARLET	21-30	10	20/30	1	0.2	500 Pulsed (CW)

The Jefferson Lab IR Demo FEL

The IR Demo installation was completed in September 1998. The injector is the critical technology for operation of systems such as this; it must produce high average currents at high brightness. Although ultimately a srf photocathode gun such as under development in Dresden [25] is believed to be the most desirable, this system utilizes a DC photocathode operating at 320 kV to produce a 37.4 MHz pulse train of 60 pC [26].

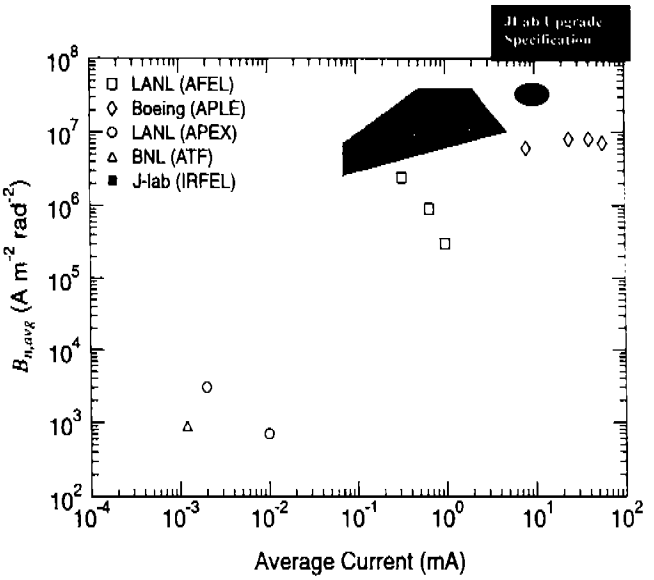

Figure 7. Adapted from [27]. The average brightness produced by a set of high current injectors. The specification of the JLab Upgrade FEL presently under construction is also shown.

This gun produces the highest average brightness of any injector gun in the world. (See Figure 7.) The cathode of this device has delivered in excess of 3 kilocoulombs from a single GaAs crystal with only occasional cleaning and recesiations [28]. It regularly delivers over 1% quantum efficiency operating in the green from a doubled YLF laser beam. The 20 ps beam is bunched by a copper fundamental cavity to around 3 ps and accelerated to 9.5 MeV in an srf cavity pair operating at 1497 MHZ. The beam is then accelerated to 36 to 48 MeV in a slightly modified CEBAF cryomodule. The beam is bent around the optical cavity mirror in a chicane, compressed by the chicane dispersion working on a slight energy slew of the micropulse and sent through the wiggler with roughly 60 A peak current in a micropulse of less than 1 ps FWHM. Approximately 0.5% of the electron beam FEL energy is extracted in the NdBFe hybrid wiggler with 40 periods of 2.7 cm. The waste beam now has a large energy spread; full width can exceed 6%. Nonetheless, the beam is brought around the second mirror in an identical chicane, then through a 180 degree arc based on the Bates design [29]. A FODO lattice brings the beam to another arc and the beam is re-injected to the accelerator in the deceleration phase of the rf. As the beam decelerates its energy spread is compressed and the resultant beam is dumped at 10 MeV, now with less than 6% full energy spread.

When operated without energy recovery the beam current is limited by rf power to 1.1 mA average producing over 300 W from the FEL. In recirculation mode the recovered beam energy permits operation to the gun HVPS average current limit of 5 mA. Figure 8 shows the measured rf power in several cavities illustrating the

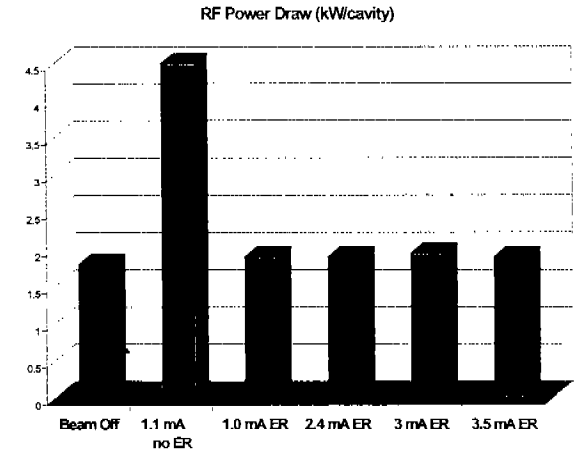

Figure 8: Measured average rf power to each linac cavity with and without energy recovery as a function of current.

independence of rf power on accelerated current. Nearly 250 kW of electron beam power is being generated from 66 kW of rf without the limitations of electron cooling time or instabilities that would occur in a storage ring system.

When optimized the laser has produced up to 1.7 kW at 3 microns in this mode. This is 150 times the average power of any other FEL in the world. The wavelength produced by the FEL is controlled by the electron beam energy. Suitable mirrors must be used for each wavelength band. To date the system has lased in three primary wavelength bands as shown in Figure 9. In addition, the system has produced 4 watts of power lasing on the fifth harmonic at 1 micron It can produce useful amounts of power at the third harmonic. Recent tests have shown the ability to produce 300 W continuously in this mode [30].

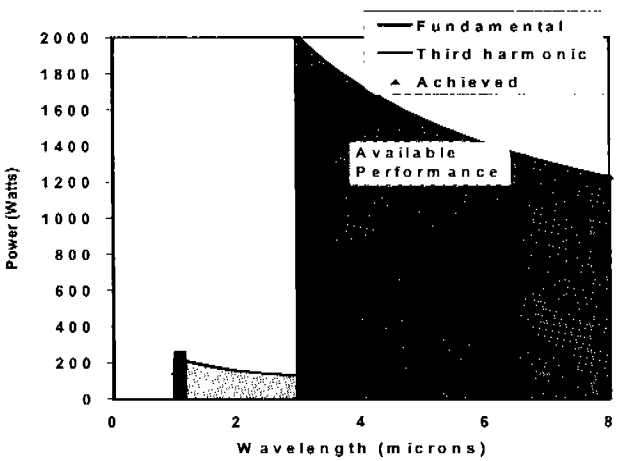

Figure 9: Projected and achieved performance of the IR Demo FEL. The full available performance can be achieved by using specialized mirrors for each wavelength band.

Building on the successful performance of the IR Demo an upgrade to the system is planned to establish shorter wavelength lasing at 1 micron and less and increase the power to 10 kW and beyond (see Figure 10). The system will be similar in layout but utilize 3 cryomodules including a new upgraded cryomodule with 40% more active length and high gradient capability. Additions of a short wavelength optimized wiggler and second optical cavity will permit high average power operation in the UV.

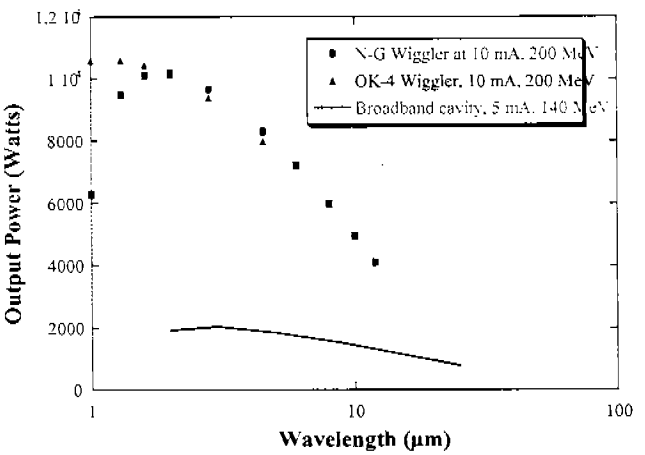

Figure 10: Projected performance of the IR Upgrade.

Additional FELs will soon offer the benefits of CW operation. An upgrade of the Stanford SCA is underway using TESLA cavities and a new refrigerator which will permit CW operation. Already one of the most productive FEL user facilities in the world, this capability with further enhance its operation for scientific research. Plans are also underway for an upgrade of the JAERI FEL to high duty factor and the construction of a machine similar to the upgraded SCA in Dresden.

4 SUMMARY

SRF technology has provided a capability for high duty factor operation of FELs that has wide ranging implications. It offers improved beam quality. It permits the use of system designs incorporating same cell energy recovery for high efficiency at high power. Its use has already permitted operation of an FEL at average power levels 150 times competing copper systems. In the future it will be incorporated into a high power SASE UV demonstration system and ultimately User facility [31]. This User facility will take advantage of the high duty factor operation to multiplex the FEL beam among many groups making practical the 4th Generation Light Source through cost sharing between many groups. It is further expected that future improvements in SRF technology will make the advantages of high duty factor operation and excellent beam quality even more compelling.

5 ACKNOWLEDGEMENT

I depended on discussions with many members of the Jefferson Lab staff in the development of this paper. I would like to especially acknowledge the contribution of Lia Merminga to perform the analysis of beam stability and the help of Peter Kneisel in reviewing the status of srf development. Errors in interpretation are my own. The break-though performance of the IR Demo FEL was the result of a team effort which I depended on and am happy to acknowledge. This work was supported by U.S. DOE Contract No. DE-AC05-84-ER40150, the Office of Naval Research, the Commonwealth of Virginia and the Laser Processing Consortium.

6 REFERENCES

[1] For a discussion of the issues see Charles A. Brau, Free-Electron Lasers, Academic Press, San Diego, 1990.

[2] S. Benson, private communication. See also G. Dattoi, et al. "Intensity Saturation Mechanism in Free Electron Lasers", IEEE J. Quant. Elect. QE-28 (1992) pgs 770-772. The overlap dependence has been added and the degradation factors normalized to one compared to the formula from this reference.

[3] G.R. Neil, S.V. Benson, M.D. Shinn, P.C. Davidson, and P.K. Kloeppel, "Optical Modeling of the Jefferson Laboratory IR Demo FEL", SPIE **2989** 160 1997.

[4] D. Douglas, "Design Considerations for Recirculating and Energy Recovering Linacs" Jefferson Lab Technical Note JLAB-TN-00-027 (November, 2000).

[5] M. Xie, "Design Optimization for an X-ray Free Electron laser Driven by SLAC Linac" Proceedings of the 1995 Particle Accelerator Conference (Dallas, 1995) pgs. 183-186.

[6] C. L. Bohn, "Recirculating Accelerator Driver for a High-Power FEL: A Design Overview", Proc. 1997 Part. Accel. Conf., IEEE Cat. No. 97CH36167, (1998) pgs 909-911.

[7] J. Kirchgessner, "Review of the Development of RF Cavities for High Currents", Proceedings from the 6th Workshop on RF Superconductivity, Newport News, VA, (1993) pgs 331-336.

[8] L. Merminga, "BBU Scaling Laws" to be published as CEBAF Tech Note.

[9] Thomas Wangler, RF Linear Accelerators, John Wiley & Sons, (1998) pg 160.

[10] C. Adolphsen, "Experimental Results and Technical Research and Development for an X-Band Linear Collider", Proc. 2000 European Particle Accelerator Conference, Vienna, Austria (2000).

[11] Hasan Padamsee, Jens Knobloch, Tom Hays, RF Superconductivity for Accelerators, John Wiley & Sons, (1998) pg 284.

[12] Donald Feldman, et al., Nucl. Instr. and Meth. in Phys. Rsch. A259 (1987) pgs 26-30.

[13] T. I. Smith, Nucl. Instr. and Meth. in Phys. Rsch. A259 (1987) pgs 1-7.

[14] G. R. Neil et al, "Sustained Kilowatt Lasing in a Free-Electron Laser with Same-Cell Energy Recovery," Phys. Rev. Letter 84(4), (2000) 662-665.

[15] J. Boyce, et al., "High Flux Femtosecond X-rays Simultaneous with FEL Infrared Pulses". submitted for publication in Science.

[16] J. Flanz, G. Franklin, S. Kowalski and C.P. Sargent, MIT-Bates Laboratory, Recirculator Status Reports, 1980 (unpublished); described in R. Rand, "Recirculating Electron Accelerators" (Harwood, New York, 1984) pp 107-109 and pg 155

[17] D. Neuffer et al., Nucl. Inst. and Meth. A **375** 123 1996.

[18] Laser Processing Consortium "Free-Electron Lasers for Industry", available from the FEL Dept. Office, Jefferson Lab, Newport News, VA. 1995.

[19] S. Benson, et al, "First Lasing of the Jefferson Lab IR Demo FEL", Nuclear Instruments and Methods in Physics Research A 409 (1999) 27-32.

[20] Campisi, I., Douglas, D., Hovater, C., Krafft, G., Merminga, L., Yunn, B., "Beam Current Limitations in the Jefferson Lab FEL: Simulations and Analysis of Proposed Beam Break-up Experiments". Proceedings of the 18th Particle Accelerator Conference (PAC 99), New York, NY, March 29-April 2, 1999.

[21] Merminga, L., Alexeev, P., Benson, S., Bolshakov, A., Doolittle, L. and Neil, G., "Analysis of the FEL-RF Interaction in Recirculating, Energy-Recovering Linacs with an FEL" Nuclear Instruments and Methods in Physics Research A 429 (1999) 58-64.

[22] D. Douglas, "Lattice Design for a High-Power Infrared FEL", Proceedings of the 1997 Particle Accelerator Conference, Vancouver, B.C., Canada, May 11-15, 1997.

[23] H. P. Freund and G. R. Neil "Free-Electron Lasers: Vacuum Electronic Generators of Coherent Radiation", Proc. IEEE Vol. 87, No. 5, (May, 1999) pgs. 782-803.

[24] W. B. Colson, "Short Wavelength free electron lasers in 1998", Nucl. Instr. and Meth. in Phys. Rsch. A429 (1999) 37-40.

[25] D. Jansen, et al., Proc. of the 1997 Particle Accelerator Conf., Vancouver, Canada (1997).

[26] D. Engwall, C. Bohn, L. Cardman, B. Dunham, D. Kehne, R. Legg, H. Liu, G. Neil, M. Shinn, C. Sinclair, "A High-DC-Voltage GaAs Photoemission Gun: Transverse Emittance and Momentum Spread Measurements", Proc. 1997 Part. Accel. Conf., (1998) pgs. 2693-2695.

[27] Dinh Nguyen, LANL, personal communication.

[28] T. Siggins et al., "Performance of the Photocathode Gun for the TJNAF FEL." Presented at the 22nd Int'l FEL Conf. To be published in Nucl. Instr. and Meth.

[29] J. B. Flanz and C. P. Sargent, "Operation of an Isochronous Beam Recirculation System," Nucl. Inst.

and Meth in Phys Research. A241 (1985) pgs 325-333.

[30] S. Benson, et al., "5th Harmonic Lasing of a FEL", Proceedings of FEL'99, to be published in Nucl. Instr. and Meth. in Phys. Rsch. (2001).

[31] A VUV free electron laser at the TESLA test facility; conceptual design report, DESY Print TESLA-FEL 95-03, Hamburg, Germany, 1995.